

Transport of Fluid Mud generated by Waves on Inclined Beds

Thijs van Kessel*, C. Kranenburg† and J.A. Battjes‡

Abstract

Liquefaction of a freshly deposited mud bed may occur if shear stresses in the bed, generated by wave-induced pressure gradients, locally exceed the yield strength. In this way fluid mud is generated, which has a concentration close to the original bed concentration (generally a few hundreds kg m^{-3}). If fluid mud is displaced, very high transport rates are to be expected. This may be an explanation for rapid mud accumulations often observed in navigation channels after storm periods. In this paper wave-induced liquefaction of a sloping mud bed is investigated with laboratory experiments. A yield strength profile of the bed is obtained with a small-scale sounding test. Rheological properties of the mud after liquefaction are determined with independent rheological experiments. It is shown that calculated shear stresses in the bed at the onset of liquefaction just exceed the measured yield strength. The combination of waves and a slope turns out to be very effective for the transport of fluid mud.

1 Introduction

Harbours and coastal areas are affected by the accumulation of mud in several respects. Resulting bathymetric changes often hamper navigation and make expensive dredging operations unavoidable in order to maintain navigable depth. Moreover, mud is often heavily polluted as it easily adsorbs many pollutants such as heavy metals and pesticides because of its high specific area and surface properties. This negatively affects water and sea bed quality and makes disposal of dredged material expensive. In order to prevent the undesired accumulation of mud, the relevant transport mechanisms have to be identified, thus providing a tool for coastal management.

*PhD Student, Hydromechanics Group, Dept. of Civ. Engrg., Delft Univ. of Technol., P.O. Box 5048, 2600 GA Delft, The Netherlands. E-mail: T.vanKessel@ct.tudelft.nl

†Assoc. Prof., Hydromechanics Group, Dept. of Civ. Engrg., Delft Univ. of Technol., P.O. Box 5048, 2600 GA Delft, The Netherlands.

‡Prof., Hydromechanics Group, Dept. of Civ. Engrg., Delft Univ. of Technol., P.O. Box 5048, 2600 GA Delft, The Netherlands.

Mud may accumulate gradually by sedimentation from the water column during slack tide. This is a slow process, as the sediment concentration in the water column generally does not exceed 1 g l^{-1} , and the settling velocity of the mud particles is low. The freshly deposited sediments may also be resuspended during ebb and flood tides, which reduces the net accumulation rate during a tidal cycle.

Another transport mechanism is the transport of concentrated, near-bottom mud layers—often referred to as 'fluid mud'—under the influence of waves and gravity. This may result in very high transport rates during a short period of time, as sediment concentrations in fluid mud may be up to a few hundreds kg m^{-3} . This transport mechanism may be an explanation for the rapid, event-like mud accumulations often observed after storm periods.

In this paper the latter mechanism is studied by means of laboratory experiments. In §2 the theory underlying the generation and transport of concentrated mud layers is discussed in greater detail; in §3 the experimental results are presented and discussed. Conclusions are drawn in §4.

2 Theory

2.1 Generation of fluid mud

Several erosion mechanisms of mud are possible. Surface erosion will occur if the bed shear stress exerted by the orbital motion of water under waves or by current, exceeds the critical shear strength for erosion (Mehta et al. 1989). Bulk erosion will occur if the shear stress inside the bed generated by wave-induced pressure gradients on the bed surface, exceeds the yield strength of the bed. For the experiments reported in this paper the latter mechanism prevailed, as the frictional bed shear stress remained small because of the absence of current.

Because of the very low permeability of a mud bed, water flow inside the bed caused by wave-induced pressure gradients is negligible (undrained conditions). Erosion caused by fluidisation or swell will not occur in this case. The behaviour during and after undrained failure of a mud layer will depend on its state of consolidation. Freshly deposited and consolidated beds tend to decrease in volume when subjected to shear, as they are loosely packed. A (positive) excess pore water pressure is generated, resulting in decreases in effective stress and strength. As the bed liquifies without the flow of water, sediment particles become mainly supported by the pore water instead of the grain skeleton. A liquified bed is easily transported if net forces are acting on it (De Wit 1995).

However, if the bed is closely packed because it has been exposed to high effective stresses in the past—by burial and subsequent exposure, for example—it tends to expand under shear, resulting in the generation of negative pore pressures. No liquefaction occurs in this case; on the contrary, the bed 'breaks'. Shear stresses needed for this type of failure to occur are generally much higher

than those for the liquefaction of loosely packed mud beds.

The sediment beds used in the experiments described in the present paper were freshly consolidated and loosely packed. Therefore, a positive excess pore water pressure generated upon failure, and liquefaction of the bed are to be expected.

The yield stress of the sediment bed is the key parameter for possible bed failure for the present experiments. It is essential that yield strength is measured *in situ*, as remoulded yield strength tends to be much lower than *in situ* strength. Measurements with a rheometer using a standard geometry in which a bed sample is injected gives erroneous results. A better option would be to use a vane geometry that inserted into the undisturbed bed, as the shear surface during insertion is different from the shear surface when measuring yield strength.

Another technique, which has been applied to the beds used in this study, is a sounding test, during which the force exerted on a small geometry slowly penetrating into the sediment bed is measured with a sensitive balance. With bearing capacity theory (Terzaghi 1943) the yield strength profile can be calculated from the force as a function of vertical position (Van Kessel 1996b).

As was remarked before, undrained failure occurs if the wave-induced shear stresses inside the mud bed exceed the local yield strength. Shear stresses in the bed generated by the pressure gradients caused by waves can be calculated from prescribed boundary conditions assuming a certain constitutive behaviour of the bed. For stresses well below the yield stress the bed will behave as an elastic material, whereas for stresses close to the yield stress the bed will behave as a visco-elastic material. Stresses beyond the yield stress result in liquefaction and concurrently viscous behaviour. If the constitutive behaviour of the bed is purely elastic, then the applied shear stress and the resulting strain are in phase. If the behaviour is purely viscous, then the shear stress and shear rate are in phase.

The wave-induced shear stresses in the bed during the present experiments were calculated assuming an elastic constitutive behaviour, which is in accordance with the concept of a yield strength as long as it is not exceeded. Horizontal and vertical displacements at the interface between sediment bed and fixed bottom were assumed to be zero (no-slip condition), whereas at the interface between sediment bed and overlying water the shear stress was assumed to be zero. The latter boundary condition can be justified if the stresses inside the bed caused by the pressure gradients are much larger than the frictional shear stress on the bed surface caused by the orbital motion of water under waves, which is shown to be true in §3.2. The final boundary condition needed to obtain a closed set of equations is the wave-induced pressure gradient exerted on the bed surface, which can be calculated from linear surface wave theory, for example. Details of the calculations are not presented herein for reasons of brevity. An analytical solution can be obtained (Van Kessel et al. 1997), which is a special case of the Yamamoto et al. (1978) model.

2.2 Transport of fluid mud

After the yield strength has been exceeded, the liquified bed starts to flow if subjected to a net force, which is the gravity force in the present study. As failure of the bed is undrained, the sediment concentration in the liquified layer equals the original bed concentration, which generally is a few hundreds kg m^{-3} . Because of the high viscosity, the flow of these layers tends to be laminar. Mixing with overlying water hardly occurs, because of the large density gradient stabilizing the interface.

In order to predict the flow of fluid mud layers, it is essential to know their rheological behaviour. The rheology of concentrated suspensions of cohesive sediment particles is quite complex; for a detailed discussion the reader is referred to Van Kessel (1996a), Toorman (1993), James et al. (1987) and Williams (1984). Fluid mud subjected to simple shear flow can be rheologically characterized by a (residual) yield strength and a shear rate dependent viscosity (non-Newtonian behaviour). A complication is that the viscosity is a function of the shear rate history rather than the actual shear rate, because structural changes that take place within fluid mud if the shear rate is changed, need time to reach an equilibrium situation. The constitutive model used to describe the fluid mud flow in the present experiments includes thixotropic behaviour (Toorman 1997):

$$\tau_{xz} = \lambda\tau_y + \left(\eta_\infty + \frac{c_1}{1 + \beta|\dot{\gamma}|} \right) \dot{\gamma} \quad (\tau_{xz} > \lambda\tau_y) \quad (1)$$

where τ_{xz} is the shear stress parallel to the bed, $\dot{\gamma}$ is the shear rate, τ_y is the yield stress, η_∞ is the viscosity as infinite shear rate and c_1 and β are coefficients incorporating shear-thinning behaviour. The structure parameter λ decreases with time from 1 to 0 as a result of structural break-up of the sediment caused by wave action (Moore 1959):

$$\frac{d\lambda}{dt} = -c_2\lambda|\dot{\gamma}| \quad (2)$$

Structural recovery is not taken into account for the present experiments, because the time scale of recovery is much larger than that of the experiments. In §3.3 the calibration of the model coefficients τ_y , η_∞ , c_1 , β and c_2 for the sediment type and concentration used is discussed.

The equation of motion for the fluid mud layer can be solved together with the rheological model and boundary conditions. The equation of motion can be simplified into:

$$\rho \frac{\partial u}{\partial t} = -\frac{\partial p}{\partial x} + \frac{\partial \tau_{xz}}{\partial z} + (\rho - \rho_w)g \sin \theta \quad (3)$$

where ρ is the density of fluid mud, ρ_w is the density of water, u the local velocity, t is time, $\partial p/\partial x$ is the the wave-induced pressure gradient, z the coordinate normal to the bed, g is the acceleration of gravity and θ is the angle of the slope

to the horizontal. The convective terms that should appear in (3) have been neglected, as for the present experiments they are very small compared to the other terms. Additionally, it has been assumed that the motion of the overlying water layer is not influenced by the mud layer, and that the slope is small. The pressure gradient at the bed caused by wave action is expressed by:

$$-\frac{\partial p}{\partial x} = -k \frac{\rho_w g a}{\cosh kh} \cos(\omega t - kx) \quad (4)$$

where k is the wave number, a is the wave amplitude, h is the water depth, ω is the circular wave frequency and x the coordinate parallel to the water surface.

Boundary conditions are:

$$\left. \begin{array}{l} z = D_1 : u = 0 \\ z = 0 : \dot{\gamma} = 0 \end{array} \right\} \quad (5)$$

Here $z = D_1$ is the elevation of the interface between non-liquified and liquified mud determined from observations and $z = 0$ is the interface between liquified mud and water. Initial conditions are:

$$t = 0 : u = 0 \text{ for all } z \quad (6)$$

These equations, which describe the motion of the mud layer after liquefaction, were solved numerically.

3 Experimental results and discussion

3.1 Experimental methods

An experimental setup was built to study wave-induced liquefaction and transport on a slope experimentally (Figure 1). Sediment beds were prepared by sedimentation and consolidation of a suspension of China clay in tap water in which 0.5% NaCl was dissolved. The initial sediment concentration was 275 kg m^{-3} . The suspension was mixed for 2 weeks in order to reach physicochemical equilibrium. China clay—mainly consisting of kaolinite—was used as an artificial mud because of its reproducible properties and easy handling. After 1 week of consolidation the bed height remained constant and the bed was tilted to its desired angle (0.05 rad). The bed height after consolidation was 0.12 m, its width 0.65 and its length 4.67 m.

At $z = 0, 0.02, 0.06$ and 0.10 m from the bed surface pore pressure transducers were mounted to observe the liquefaction behaviour. These transducers were located at measuring station 3. The sediment concentration profile in the bed was measured with a conductivity probe. Velocities both in the bed (after liquefaction) and above the bed were measured with two electromagnetic flow meters (EMF) mounted on traversing units to obtain vertical profiles. These traversing units were located at measuring stations 1, 2 and 3. Sediment concentrations in

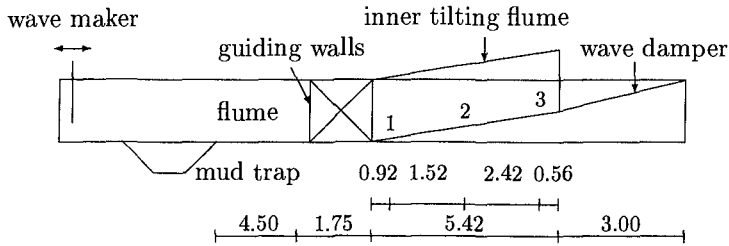


Figure 1: Experimental set-up (not to scale); measuring stations 1, 2 and 3 are indicated; lengths in m

the water column were measured with turbidity meters in order to estimate the importance of interfacial mixing. Also three wave height meters were installed. The signals of these instruments were logged onto a PC.

3.2 Wave-induced liquefaction

The experiments were started by generating sinusoidal waves with a period of 1.65 s and an initial wave amplitude of 0.005 m. During the experiments the wave amplitude was increased in steps to 0.008, 0.010, 0.013, 0.016, 0.021, 0.027, 0.036 and finally 0.042 m and the pore pressure response was measured (Figure 2). Initially no changes in the wave-averaged pore pressure were observed. However, after an increase in wave-height from $a = 0.005$ to $a = 0.008$ m, suddenly excess pore pressures were generated and the bed started to liquefy. Bed flow does not yet occur at this wave-height, as is illustrated in Figure 3, where the velocity histories at several levels inside and above the bed are shown.

The bed did flow if the wave amplitude was increased to 0.010 m. This can be derived from Figure 2, where a sudden drop in pore pressure can be attributed to the removal of the liquified mud layer. The thickness of this layer can be calculated from the observed pore pressure drop (approximately 150 Pa at $z = 0.06$ m), as the initial sediment concentration is known from the conductivity probe measurements ($\rho = 1340 \text{ kg m}^{-3}$). The thickness thus estimated is 0.045 m. This result is consistent with Figure 4, where the velocity histories shown indicate that the bed is eroded up to the level $z = 0.065$ m.

A comparison of the wave-induced stresses in the bed—calculated from the elastic model—with the yield strength profile obtained with the sounding test (§2) is shown in Figure 5. At $a = 0.005$ m, when no liquefaction is observed, wave-induced shear stresses just remain below the yield strength. At $a = 0.008$ m, however, onset of liquefaction was observed, which is consistent with Figure 5, where, for this wave amplitude, the shear stress exceeds the yield strength in the

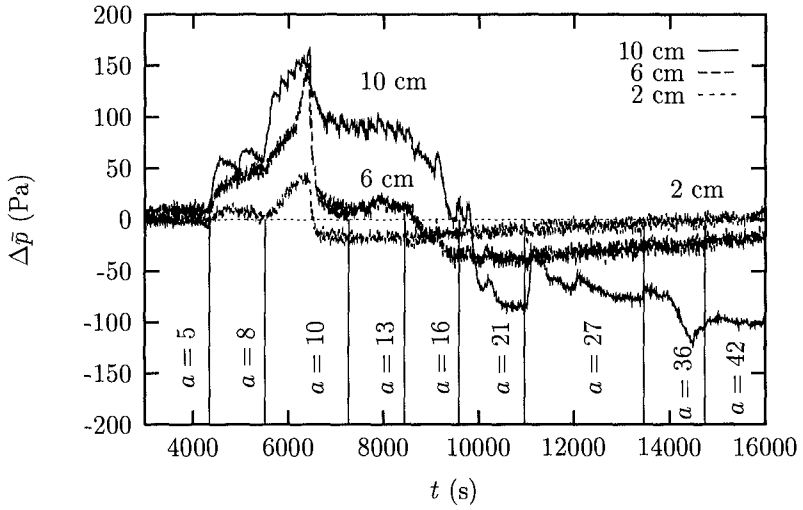


Figure 2: Changes in wave-averaged pore pressure $\Delta\bar{p}$; wave amplitudes in mm

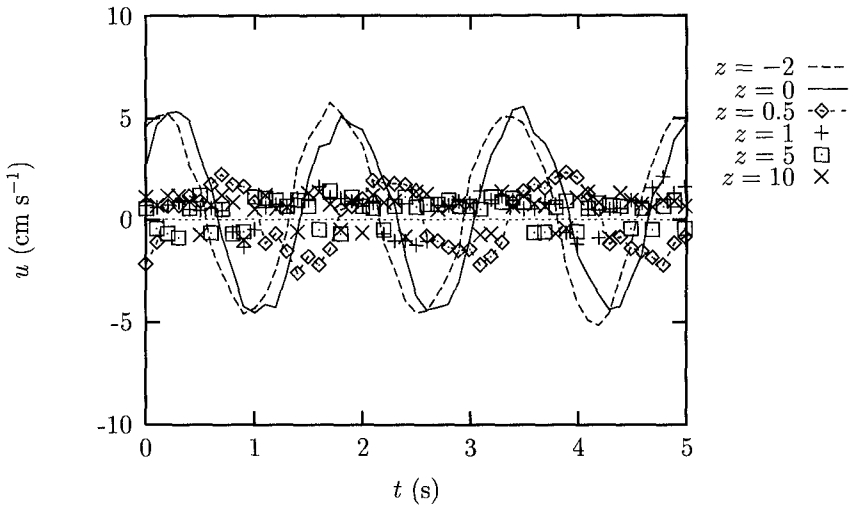


Figure 3: Velocities versus time for $a = 5$ mm; z in mm; station 3

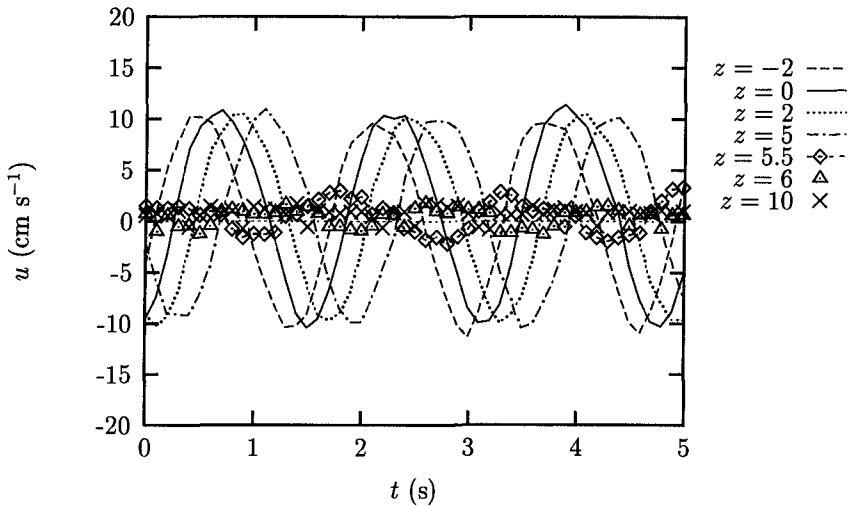


Figure 4: Velocities versus time for $a = 26$ mm; z in mm; station 3

upper 8 cm of the bed. The onset of liquefaction can therefore be well predicted if the yield strength profile of the bed is known. The yield strength of the bed increased with depth in a similar fashion as the effective stress, which was also observed by Bowden (1988).

3.3 Fluid mud flow

After liquefaction the fluid mud starts to flow. Rheological properties of China clay have been investigated independently to calibrate the rheological model applied (§2). In Figure 6 the equilibrium flow curve of China clay with $C = 467$ kg m^{-3} suspended in tap water with 0.5% NaCl is shown. It was measured with a Carrimed controlled stress rheometer equipped with a cone-plate geometry. This flow curve has been used to calibrate the Toorman (1997) model. In addition to measuring the flow curve, also thixotropic experiments have to be performed to measure the time-scales of structural break-up. These measurements are not discussed herein, the reader is referred to Van Kessel (1996a). Values for the model parameters used are listed in Table 1.

With the rheological model and the equation of motion presented in §2 fluid mud flow can be calculated numerically. Results of these calculations are shown in Figure 7. Peak velocities are approximately 0.02 m s^{-1} and increase in time because of structural break-up of fluid mud. Plug flow can be explained by the residual yield strength of the bed; negative velocities do not occur for the conditions during the experiments because of the finite yield stress. The model shows that the combination of wave-loading and the shear-thinning behaviour of mud results in a decrease in its effective viscosity, which markedly enhances

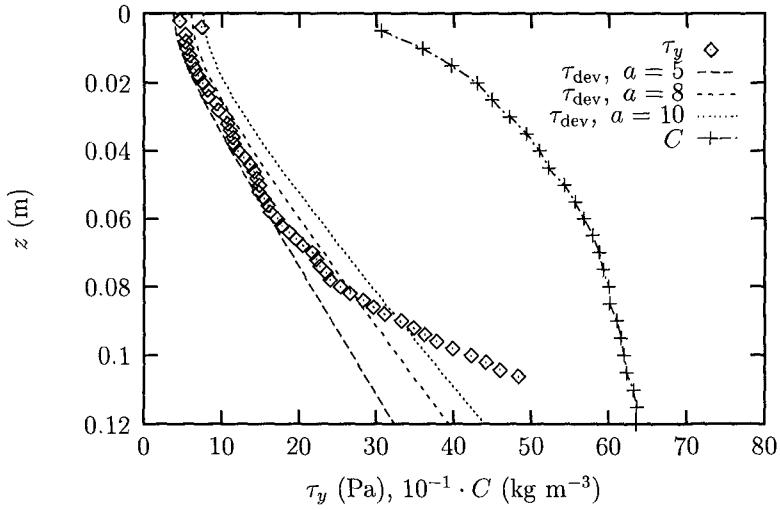


Figure 5: Yield strength, deviator stress and concentration profiles of a bed of China clay, obtained from sedimentation of a suspension of 275 kg m^{-3}

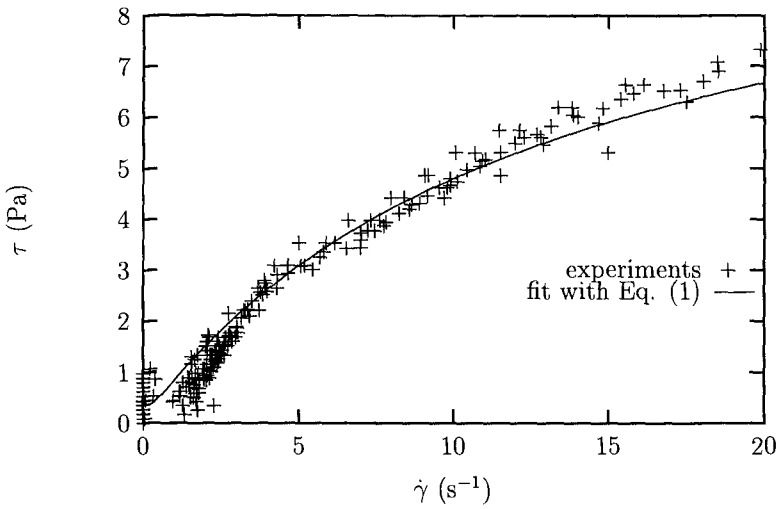


Figure 6: Equilibrium flow curve for China clay; $C = 467 \text{ kg m}^{-3}$, with Carrimed controlled stress rheometer; cone-plate configuration used

Table 1: Calibrated values of the parameters in (1) based on Figure 6 and τ_y shown in Figure 5

parameter	value	dimension
τ_y	$3.4 + 235z$	Pa (z in m)
η_∞	0.0066	Pa s
c_1	0.86	Pa s
β	0.081	s
c_2	10^{-2}	-

transport under the influence of net forces, such as gravity.

A displacement of 5 m (approximately the length of the test section) is reached within a few minutes, therefore fluid mud flow can be observed only for a short period of time, which is confirmed by visual observations. However, quantitative comparison between the flow model and measured velocities proved difficult. The accuracy of the flow meters in the velocity range of 0.01 m s^{-1} is low, too.

After removal of the fluid mud layer, a new non-liquefied layer became exposed, which would only liquefy if the wave amplitude was increased. At $a = 0.027 \text{ m}$, when the bed is clearly completely eroded at $z = 0.06 \text{ m}$, a pore pressure increase at $z = 0.10 \text{ m}$ was observed. Erosion of this layer occurred at $a = 0.027$ and 0.036 m .

Even at the largest wave amplitude, $a = 0.042 \text{ m}$, not all sediment was liquefied. After the experiments a layer of $0.02\text{--}0.03 \text{ m}$ was still present in the upper part of the tilting flume, which is not influenced by the sill at the lower end. This can be explained by two factors. First, the yield strength close to to the fixed bottom is the highest as the mud has been most compacted by the weight of the overlying sediment, and secondly, the (high) pressure gradients at the end of the experiments are much less effective, as the bed becomes thinner and thinner, which leads to lower shear stresses inside the bed.

4 Conclusions

Undrained failure of freshly deposited mud layers may be caused by pressure gradients on the bed surface, if the resulting shear stresses inside the layer locally exceed the yield strength. If the yield strength profile is known, failure can be well predicted using an elastic model to calculated shear stresses in the mud layer. For loosely packed layers, which have not yet been subjected to higher effective stresses than the actual effective stress, positive excess pore pressure are generated upon failure and liquefaction occurs. The strength of the layer is then much reduced, and a transition from predominantly elastic to predominantly viscous behaviour takes place.

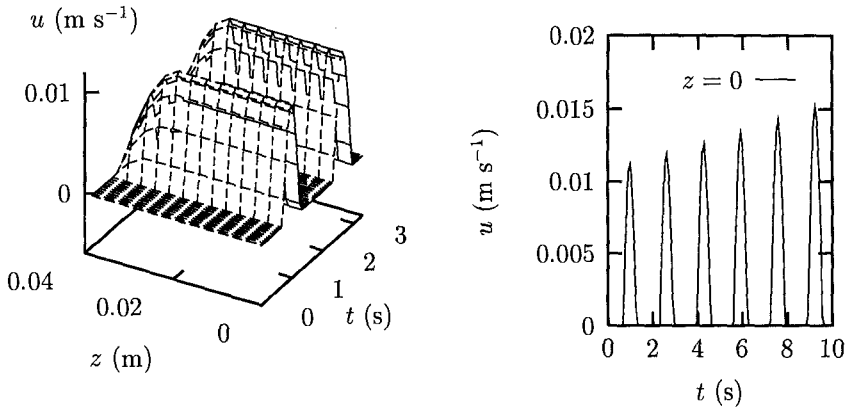


Figure 7: Velocity profile $u(z, t)$ resulting from wave-induced liquefaction on a slope. $D_1 = 0.04$ m, $\rho = 1346$ kg m $^{-3}$, $\theta = 0.05$ rad, $h = 0.30$ m, $a = 10$ mm, $k = 2.49$ m $^{-1}$, $\omega = 3.93$ s $^{-1}$; rheological coefficients used are listed in Table 1

If the fluid mud layer generated by liquefaction starts to flow under the influence of a net force, e.g. gravity, very high transport rates in a short period of time are possible, as the concentration of the liquified mud equals the original bed concentration (generally a few hundreds kg m $^{-3}$). This may partly explain the large mud accumulations often observed in the field after a storm period. In order to model fluid mud flow, its rheological properties have to be studied first, taking into account shear rate dependent and thixotropic behaviour.

The transport mechanism described in this paper may be important for the redistribution of cohesive sediments in depositional areas, where layers of freshly deposited, still consolidating mud are present. In erosional areas, however, the surface layer has generally been buried in the past and is therefore more compacted. Also ageing effects will contribute to the strength which tends to be much higher than for surface layers in depositional areas. Liquefaction of these old layers is therefore unlikely.

Acknowledgments

This work was carried out as part of the G8 Coastal Morphodynamics program. It was funded jointly by the Delft University of Technology and the Commission of the European Communities, Directorate General for Science, Research and Development under contract no. MAS2-CT-92-0027. It was carried out in the framework of the Dutch Center for Coastal Research. Special thanks go to

M. Reijnders, who assisted in the measurements reported.

References

- Bowden, R. (1988). *Compression behaviour and shear strength characteristics of a natural silty clay sedimented in the laboratory*. Ph. D. thesis, Oxford University.
- De Wit, P. (1995). *Liquefaction of Cohesive Sediments caused by Waves*. Ph. D. thesis, Delft University of Technology, the Netherlands.
- James, A., D. Williams, and P. Williams (1987). Direct measurement of static yield properties of cohesive suspensions. *Rheol. Acta* 26, 437–446.
- Mehta, A., E. Hayter, W. Parker, R. Krone, and A. Teeter (1989). Cohesive sediment transport. I: Process description. *J. Hydraul. Eng.* 115(8), 1076–1093.
- Moore, F. (1959). The rheology of ceramic slips and bodies. *Trans. Brit. Ceram. Soc.* 58, 470–494.
- Terzaghi, K. (1943). *Theoretical Soil Mechanics*. John Wiley and Sons, New York.
- Toorman, E. (1993). *Rheological properties*. In: On the methodology and accuracy of measuring physico-chemical properties to characterize Cohesive Sediments. MAST-I Report. pp. 79–123.
- Toorman, E. (1997). Modelling the thixotropic behaviour of dense cohesive sediment suspensions. *Rheologica Acta*, (to be publ.).
- Van Kessel, T. (1996a). Rheological properties of cohesive sediment suspensions. Report 1–96, Hydromechanics Group, Delft University of Technology, the Netherlands.
- Van Kessel, T. (1996b). Small-scale sounding tests on soft saturated cohesive soils. Report 7–96, Hydromechanics Group, Delft University of Technology, the Netherlands.
- Van Kessel, T., C. Kranenburg, and J. Battjes (1997). Wave-induced liquefaction and transport of mud on inclined beds. (to be publ.).
- Williams, D. (1984). *Rheology of cohesive suspensions*, Volume 14 of *Lecture notes on coastal and estuarine studies*.
- Yamamoto, T., H. Koning, H. Sellmeijer, and E. Van Hijum (1978). On the reponse of a poro-elastic bed to water waves. *Journal of Fluid Mechanics* 87(1), 193–206.